NATIONAL ADVISORY COMMITTEE FOR AERONAUTICS

TECHNICAL NOTE 4164

TWO-DIMENSIONAL DIFFUSION THEORY ANALYSIS OF REACTIVITY EFFECTS OF A FUEL-PLATE-REMOVAL EXPERIMENT

By Edward R. Gotsky, James P. Cusick, and Donald Bogart

Lewis Flight Propulsion Laboratory
Cleveland, Ohio

Washington
January 1958

NATIONAL ADVISORY COMMITTEE FOR AERONAUTICS

TECHNICAL NOTE 4164

TWO-DIMENSIONAL DIFFUSION THEORY ANALYSIS OF REACTIVITY EFFECTS OF A FUEL-PLATE-REMOVAL EXPERIMENT

By Edward R. Gotsky, James P. Cusick, and Donald Bogart

SUMMARY

Two-dimensional two-group diffusion calculations were performed on the NACA reactor simulator in order to evaluate the reactivity effects of fuel plates removed successively from the center experimental fuel element of a seven- by three-element core loading at the Oak Ridge Bulk Shielding Facility. The reactivity calculations were performed by two methods: In the first, the slowing-down properties of the experimental fuel element were represented by infinite media parameters; and, in the second, the finite size of the experimental fuel element was recognized, and the slowing-down properties of the surrounding core were attributed to this small region. The two calculation methods agreed reasonably well with the experimental reactivity effects.

INTRODUCTION

The NACA Lewis laboratory is interested in a high-flux research reactor with which the components of high power density reactors under development for various flight applications can be studied. The reactor being considered employs an array of aluminum fuel elements similar to those of the Materials Testing Reactor in Idaho.

The geometric center of the active lattice of a reactor is an attractive location for experiments because of high flux and flux symmetry. The geometric center of the core, however, is also the most sensitive reactivity region for accidental compositional changes, and great care must be exercised in the design of such in-pile experiments. Many reactivity calculations have been made for both fueled and unfueled experiments in a center test hole in support of the design of the NACA research reactor. Since reactivity calculations are subject to uncertainty, an experimental program with the Bulk Shielding Reactor at Oak Ridge National Laboratory was initiated in order to evaluate the methods of analysis. In these Oak Ridge experiments, the core configuration of the

NACA research reactor was mocked up within the limits of excess reactivity and materials available to the Bulk Shielding Reactor. The loading was such that the reactivity effects of voids within the core could be measured and the worth of fuel-element water passages and fuel-element plates could be determined. The Bulk Shielding Reactor is fully discussed in reference 1. The unpublished experimental data for this particular loading were obtained at the Oak Ridge National Laboratory by E. B. Johnson, K. M. Henry, J. D. Kingdon, and T. M. Hallman.

The experiments in which the reactivity effects are measured are conveniently analyzed by group diffusion calculations. Within the limits of diffusion theory, two- and three-group analyses yield reasonable neutron flux distributions for thermal and epithermal reactors. For hydrogen-moderated reactors, many modified group diffusion methods have been used to interpret criticality experiments (refs. 2, 3, and 4).

The present paper is concerned with the Bulk Shielding Reactor fuel-plate-removal experiments and the correlation of these data with diffusion theory calculations. These experiments have been analyzed by two-group two-dimensional diffusion calculations. The solutions have been obtained on a two-dimensional nuclear-reactor simulator that is based on the design of the simulator described in reference 5.

The cooperation of the Oak Ridge National Laboratory and the staff of the Bulk Shielding Facility in performing the reactivity experiments is gratefully acknowledged. The authors are greatly indebted to Miss Dorothy Hood, who supervised the calculations on the reactor simulator.

REACTOR AND REACTIVITY EXPERIMENTS

The Bulk Shielding Reactor is an assembly of fuel elements that may be arranged into various critical configurations. The fuel is highly enriched uranium contained in aluminum-clad fuel plates. A complete fuel element is made up of 18 fuel plates and contains a total of about 140 grams of uranium-235.

Reactor Loading

The reactor configuration used in the reactivity experiments is shown schematically in figure 1. The loading consisted of 21 fuel elements in a seven-by-three array with beryllium oxide (BeO) reflector pieces arranged in one row on the north and two rows on the south. The east and west faces of the core were reflected by water and permitted complete insertion or complete withdrawal of the two guillotine safety blades. Each safety blade consisted of a thin cadmium sheet between two aluminum plates approximately 12 by 24 inches. The guillotine safety

blades were guided and positioned, relative to the core, by grooved aluminum pieces and were supported by electromagnets actuated by scram circuits. A regulating rod and a core safety rod were provided in the control-rod fuel elements in grid positions 23 and 27, respectively.

The regulating-rod calibration was obtained by the method of distributed poisons for three configurations of the guillotine safety blades: namely, both guillotines out, number 1 guillotine out with number 2 guillotine in, and both guillotines in. The elements through which the conventional safety rod and the regulating rod move contained half the normal number of fuel plates and, therefore, about 70 grams of uranium-235 each. The primary-reflector elements were hot-pressed beryllium oxide blocks encased in watertight aluminum cans of the same outer dimensions as the fuel elements. The reactor was moderated and cooled by water that also served as the secondary reflector and reactor shield. The center grid position 25 was occupied by the experimental fuel assembly.

It should be noted that this core loading had vertical symmetry about the horizontal midplane and, in addition, east-west symmetry about a vertical plane across the narrow core dimension. (Although the top and bottom reflectors were not identical, the reactor was symmetrical nuclearwise because the top and bottom reflectors were predominantly water.) The vertical symmetry permits a typical horizontal slice through the reactor to be analyzed. Because of symmetry within the plane of this horizontal slice, only one-half of this slice must be simulated for diffusion calculations. An additional calculation indicated that the effect of the partially inserted core control rod does not significantly affect the flux distributions at the center grid position (25).

Removable-Fuel-Plate Assembly

In the reactivity experiments discussed in this report, grid position 25 was occupied by a standard fuel element in which only 6 of the 18 curved fuel plates were brazed into the grooved side plates. A photograph of this removable-fuel-plate assembly is shown in figure 2. The fuel plates are removable with the exception of the two end plates and the four plates blocked by the fuel-element handle. The plates are 60 mils thick, and the water passages are 117 mils thick; the fuel element is 24 inches long and 3 inches wide.

These fuel plates were removed in two sequences. In sequence I, the interactions were maximized by successively removing adjacent fuel plates and thereby forming an enlarging water region near the center of the core. In sequence II, the interactions of each plate removed were initially minimized by removing plates farthest apart from each other.

These sequences are illustrated in figure 3, in which letters A to L represent the fuel plates removed in each step.

Experimental Results

The reactivity per incremental fuel plate removed in the maximum interaction (sequence I) and in the minimum interaction (sequence II) is presented in figure 4. The net effect of the removal of fuel plates and the consequent enlargement of water regions decreased the reactivity in all cases. The reactivity for each fuel plate removed was greatly affected by the sequence of removal. In sequence I, for example, the worth of adjacent fuel plates increased rapidly as the region devoid of fuel enlarged. On the other hand, in sequence II, individual fuel plates from opposite sides of the element had equal worth, while the worth of fuel plates from intermediate positions in the element increased slowly at first.

In these removable-fuel-plate sequences, available core excess reactivity permitted 11 fuel plates to be removed. In the maximum interaction, removal of the twelfth plate (number D in fig. 4(a)) shut down the reactor when the plate was 45-percent withdrawn from the core. At this point, the regulating rod was fully withdrawn from the core; this indicated that the withdrawn portion of the twelfth fuel plate was worth 0.16 $\Delta K/K$ percent. (Symbols are defined in appendix A.) The accumulated reactivity of the first 11 fuel plates was 2.36 percent. The complete twelfth fuel plate is estimated to be worth at least $0.16/0.45 = 0.36$ $\Delta K/K$ percent (shown in fig. 4(a) as a tailed data point). In the minimum interaction, the worth of the twelfth fuel plate is readily estimated by subtracting the cumulative reactivity of sequence II, step 11, from the cumulative reactivity of sequence I, step 12. A reactivity of 0.48 $\Delta K/K$ percent was obtained, as shown in figure 4(b) as a tailed data point.

The cumulative reactivity of these sequences is presented in figure 5 as a function of the number of fuel plates removed (each fuel plate contains 7.78 g of uranium-235). The minimum-interaction sequence was used as a basis for the reactivity calculations reported herein and for the comparison between the analytical group diffusion results and the experimental data.

GROUP DIFFUSION CALCULATIONS ON REACTOR SIMULATOR

The Simulator

The NACA two-dimensional reactor simulator is an analogue computer for obtaining solutions to the neutron-group diffusion equations.

Reactivity problems in which spatial symmetry exists in only one dimension may be solved. The simulator is a direct extension of the one-dimensional device in use at the NACA Lewis laboratory since 1951 (ref. 5).

The two-dimensional reactor simulator is shown in figure 6. The fast- and thermal-neutron-group resistor-network boards, in which the space-point resistors for a particular problem are prefabricated in aluminum plug-in units, may be seen on the right. The source-input panels are shown on the left. The problem is iterated from group to group by varying the source input until a converged flux distribution and value of the effective multiplication factor K_{eff} are obtained. In the two-group formulation used, epithermal fission and absorption are part of the fast-group processes.

Simulator Representation of Loading

The core loading shown previously had vertical symmetry about the horizontal midplane and, in addition, symmetry about a vertical plane across the narrow core dimension. The vertical symmetry permits a typical horizontal slice through the reactor to be analyzed. Because of symmetry within the plane of this horizontal slice, it is necessary to simulate only half of this slice for the diffusion calculations. Representation of this geometry on the reactor simulator, therefore, takes the form shown in figure 7, where the core fuel elements, the primary beryllium oxide reflectors, and the secondary water reflector are viewed from above. The fuel element in the central core position, from which fuel plates were successively removed, is shown in the inset. There is a net point for each area shown. Each coarse net point has the dimensions of a fuel element, about 3 inches square. The medium-sized net points are one-fourth of the coarse grid size. The area at the center of the core represents one-half of the experimental fuel element from which fuel plates were individually removed. In order to obtain a detailed description of the fluxes in this region, fine-sized net points that represent areas about a centimeter on a side were used. In all, the calculation involved 69 coarse net points, 34 medium net points, and 32 fine net points in each group of the two-group solution. The nuclear properties used for each space point are for the homogenized contents of the experimental region represented.

Two-Group Formulation

The two-group multiregion flux equations and a brief description of the methods of evaluating group parameters are given in appendix B. The two-group constants used in these calculations for the unperturbed

core are shown in table I. These parameter values are similar to those used to predict reactivity effects in the early Materials Testing Reactor (Idaho) loadings, where fuel elements similar to those in the Bulk Shielding Reactor were used. In the two-group formulation used here, epithermal fission and absorption are retained as part of the fast-group processes; this requires the use of the fast multiplication constant K_f and the nonabsorption probability p_{th}. It is shown in reference 6 that a two-group formulation including epithermal absorption and fission as used herein predicts reactivities that agree with a formulation which considers in detail the energy-dependent nuclear processes in the epithermal region. Values of L_f^2 and L_{th}^2 are derived from experimental values for metal-water mixtures; and other nonthermal values are calculated from slowing-down distributions in infinite media regions of the same composition. Parameter values for regions in the center fuel element with fuel plates removed were estimated in this manner also.

In all cases, the neutron leakage in the direction normal to the plane of the two-dimensional solution is assumed proportional to the local flux with the vertical geometric buckling B_z^2 as the constant of proportionality. The B_z^2 value of 0.001622 is based on an actual core height of 62.0 centimeters plus reflector savings of 16.6 centimeters due to the aluminum-water regions above and below the core. The problem of keeping this vertical buckling constant as more and more fuel plates are removed accounts for part of the small discrepancy between experiment and calculations.

The question immediately arises as to the validity of diffusion theory in regions that are geometrically small, such as regions where a few fuel plates have been removed. For example, removal of two adjacent fuel plates results in a water passage that is about 1 by 7 centimeters in cross section and runs the full core height. The slowing-down properties of such a small region can hardly be characterized by the slowing-down length in water, which is about 5.6 centimeters. It is reasonable to assume that the slowing-down properties of the surrounding core may be more significant. For this reason, the diffusion calculations for each core configuration were performed twice; first, using the homogeneous diffusion properties for each region regardless of size (referred to hereafter as "local region slowing-down" cases); and second, using the values of L_f^2 and p_{th} for the surrounding core to characterize the slowing down with absorption in the regions where fuel plates were removed (referred to as "surrounding region slowing-down" cases). In the surrounding region slowing-down cases, two-group constants other than L_f^2 and p_{th} were based on the local region properties.

Experimental Configurations Calculated

Calculations of the reactivity effects resulting from fuel-plate removal were performed for the reference core with no fuel plates removed and for the minimum interaction sequence in which 6, 10, and the equivalent of 13.5 fuel plates were removed from the center fuel element. The fine-grid-point arrangement used in each case duplicated compositionally the experimental geometry within the limits of the 32 space points available. An additional case, in which the range of the experimental data was extended by removing all 18 plates of the central fuel element, was calculated in order to estimate the worth of one complete fuel element at the center of the core.

CALCULATED RESULTS

Unperturbed Core

The representative two-dimensional flux distributions are shown in figure 8 for the unperturbed core with no fuel plates removed from the center fuel element. Figure 8(a) shows the integrated fast-flux distribution in the core and reflectors. The magnitude of the fluxes is shown relative to a spatial average core thermal-neutron flux of unity. Figure 8(b) shows the thermal-neutron flux distribution with characteristic peaking in the reflectors and falloff toward the corners of the slab. There is an over-all asymmetry due to the thicker primary reflector on one face of the core.

To observe the effects of fuel-plate removal from the central fuel element, the flux distributions across the narrow core dimension where maximum perturbations occur are noted. Reactivity effects were evaluated by integrating the two-dimensional flux distributions obtained over the core volume.

On an absolute basis, the value of K_{eff} for this Bulk Shielding Reactor core loading was observed experimentally to be 1.025; that is, the loading had 2.5-percent excess reactivity. The value of K_{eff} estimated from two-dimensional diffusion calculations is 1.032, an estimated excess reactivity of 3.2 percent.

Local Region Slowing-Down Model

Neutron flux distributions for several local region slowing-down cases are shown in figure 9. The flux distributions across the narrow core dimension are shown for three cases: (1) the unperturbed core, (2) 10 fuel plates removed, and (3) all 18 fuel plates in center fuel

element removed. The fluxes are relative to a spatial average thermal flux of unity in the core. Shown in figure 9 are data for the core with the central fuel element, the beryllium oxide side reflectors of different thicknesses, and the secondary water reflectors. Removal of the fuel plates and, therefore, fast-neutron sources, with consequent replacement by water, has reduced the fast flux φ_f for a large region in the vicinity of the central fuel element by providing a large internal slowing-down region. The thermal fluxes φ_{th} are consequently built up in this region. The overflow of neutrons diffusing into surrounding fuel elements is felt for about two thermal-diffusion lengths into the core, after which the thermal fluxes are unperturbed. The reactivity worth of remaining center fuel plates and of plates in adjoining elements is increased as a result. The net reactivity effect is the sum of the $-\Delta K$ due to fuel-plate removal and the $+\Delta K$ due to adjoining fuel plates operating in higher thermal fluxes.

Surrounding Region Slowing-Down Model

Figure 10 illustrates the two-group neutron fluxes for 10 fuel plates removed, as calculated by assuming the values of L_f^2 and p_{th} for the missing-fuel-plate region to be the same as those of the surrounding core. These flux distributions are compared with the fluxes for the unperturbed core. The slowing-down parameter L_f^2 for the core is larger than the value of L_f^2 for the missing-fuel-plate region, with the result that fewer neutrons slow down in this central region. Consequently, the thermal-neutron flux at the center region for this surrounding region slowing-down case is lower than the thermal-neutron flux for the corresponding local region slowing-down case. The remaining fuel plates in the center test element and in the adjoining elements, being in regions of lower thermal flux for the surrounding region slowing-down case, are worth less than the fuel plates for the local region slowing-down case, where thermal flux is higher. Inasmuch as the net reactivity effect is the sum of the $-\Delta K$ due to fuel-plate removal and the $+\Delta K$ due to adjoining fuel plates operating in higher relative thermal fluxes, quite different effects may be expected from the two diffusion calculations.

DISCUSSION

The net reactivity effects of fuel-plate removal from the center fuel element, as measured at the Bulk Shielding Reactor and as presently calculated, are compared in figure 11. The local region slowing-down calculations consistently underestimate the observed reactivity effects. On the other hand, the surrounding region slowing-down calculations predict

larger reactivity effects for fuel-plate removal up to about 10 plates, so that the actual physical situation is bracketed.

Both calculations underestimate an extrapolation of the experimental data corresponding to removal of the remaining fuel plates in the center fuel element. This may indicate that a third-dimensional effect is becoming important. In all of the present calculations, neutron leakage in the vertical direction, that is, normal to the plane of solution, was taken to be proportional to the local flux φ with a fixed value of the vertical geometric buckling B_z^2 as the constant of proportionality. This assumes a cosine flux distribution in the z-direction above and below the plane of solution. Furthermore, this assumption implies that the flux in any horizontal plane is directly proportional to the flux in the horizontal midplane.

As the missing-fuel-plate region at the center of the core enlarges, however, an increasingly important diffusion region with reflector properties is provided; this gives rise to a nonuniform flux distribution above and below the plane of solution. This internal water region acts essentially as a fast control rod by collecting fast neutrons over a relatively large range of several fast diffusion lengths in the core, by moderating, and then by diffusing them back into the core as thermal neutrons over a shorter range of several thermal diffusion lengths.

To illustrate this third-dimensional effect, consider figure 12, in which portions of the center fuel element are removed from the top and bottom of the core and replaced with water. This internal reflector (water) gathers in fast neutrons from all directions over a range of about one fast-transport mean free path in the core (4 cm) and moves the neutrons away from the center of the core. These neutrons are thermalized in the water region and diffuse into the core over a range of about one thermal-transport mean free path (0.8 cm). The net result is a transfer of fast neutrons away from the center of the core to regions of less importance. As the internal-reflector region increases in height, the migration of fast neutrons away from the core center also increases.

The two-dimensional diffusion calculations cannot account for this fast-neutron migration away from the center of the core, and therefore higher thermal fluxes are indicated in the central core region than are present in the experiment. The reactivity worth of the fuel elements surrounding the central fuel element are consequently overestimated, and the worth of the central fuel element is underestimated.

An approximation of the diffusion in the internal water region can be made by decreasing the effective average height of the core; this results in an increase in B_z^2 and a consequent increase in the vertical leakage term $D_f B_z^2$. To illustrate this, a reduction in effective core

height of 1 centimeter results in a decrease in reactivity of 0.3 percent ΔK for this core loading. (The reduction in reactivity is linear for about 6 cm in effective core height.)

CONCLUSION

The three-dimensional reactivity effects measured in the Bulk Shielding Reactor core-loading experiments are approximated by a two-dimensional calculation. Over the range of experimental data, the two-dimensional diffusion calculations predict reactivity effects that bracket the experimental data reasonably well.

Lewis Flight Propulsion Laboratory
National Advisory Committee for Aeronautics
Cleveland, Ohio, October 18, 1957

APPENDIX A

SYMBOLS

B_z^2	buckling in direction normal to plane of solution
D	diffusion coefficient
h	height of active lattice
K	multiplication constant
K_{eff}	effective multiplication factor for reactor
L_f^2	mean-square slowing-down length for fission neutrons
L_{th}^2	mean-square diffusion length for thermal neutrons
p_{th}	fraction of absorbed neutrons escaping capture in slowing down
δ_1	top reflector savings
δ_2	bottom reflector savings
Σ_A	macroscopic absorption cross section
Σ_F	macroscopic fission cross section
Σ_{Sl}	macroscopic slowing-down cross section
ν	number of neutrons emitted per fission
φ	neutron flux

Subscripts:

f	fast neutron group
th	thermal neutron group

APPENDIX B

DIFFUSION EQUATIONS AND GROUP CONSTANTS USED IN REACTIVITY CALCULATIONS

Equations

Two-group multiregion two-dimensional diffusion calculations are based on the following flux equations that include effects of fast absorption and fission:

$$D_f\left(\frac{\partial^2}{\partial x^2}+\frac{\partial^2}{\partial y^2}\right)\varphi_f-(\Sigma_{A,f}+\Sigma_{Sl,f}+D_fB_z^2)\varphi_f+\nu\Sigma_{F,f}\varphi_f+\nu\Sigma_{F,th}\varphi_{th}=0 \tag{B1}$$

$$D_{th}\left(\frac{\partial^2}{\partial x^2}+\frac{\partial^2}{\partial y^2}\right)\varphi_{th}-(\Sigma_{A,th}+D_{th}B_z^2)\varphi_{th}+\Sigma_{Sl,f}\varphi_f=0 \tag{B2}$$

In equations (B1) and (B2), effective absorbers are introduced to account for neutron leakage in the direction normal to the plane of solution; these are $D_fB_z^2$ and $D_{th}B_z^2$ for the epithermal and thermal groups, respectively. The quantity B_z^2 is the geometric buckling given in terms of the equivalent bare-core dimensions in the direction normal to the plane of solution. For the present reactor,

$$B_z^2=\frac{\pi^2}{(h+\delta_1+\delta_2)^2}$$

Inasmuch as the macroscopic cross sections are the effective averages in each energy group, the mean-square slowing-down length L_f^2 and the mean-square thermal diffusion length L_{th}^2 may be defined as

$$L_f^2=\frac{D_f}{\Sigma_{A,f}+\Sigma_{Sl,f}} \tag{B3}$$

$$L_{th}^2=\frac{D_{th}}{\Sigma_{A,th}} \tag{B4}$$

The fraction of absorbed neutrons escaping capture in slowing down (p_{th}) also may be expressed in terms of these effective values as

$$p_{th} = \frac{\Sigma_{Sl,f}}{\Sigma_{A,f} + \Sigma_{Sl,f}} \tag{B5}$$

The multiplication constants representing the number of neutrons born per neutron absorbed in each group are

$$K_f = \nu \frac{\Sigma_{F,f}}{\Sigma_{A,f}} \tag{B6}$$

$$K_{th} = \nu \frac{\Sigma_{F,th}}{\Sigma_{A,th}} \tag{B7}$$

With these definitions, two-group equations (B1) and (B2) may be rewritten as:

$$D_f \left(\frac{\partial^2}{\partial x^2} + \frac{\partial^2}{\partial y^2}\right)\varphi_f - \left(\frac{D_f}{L_f^2} + D_f B_z^2\right)\varphi_f + K_f (1 - p_{th}) \frac{D_f}{L_f^2} \varphi_f + K_{th} \frac{D_{th}}{L_{th}^2} \varphi_{th} = 0 \tag{B8}$$

$$D_{th}\left(\frac{\partial^2}{\partial x^2} + \frac{\partial^2}{\partial y^2}\right)\varphi_{th} - \left(\frac{D_{th}}{L_{th}^2} + D_{th} B_z^2\right)\varphi_{th} + p_{th} \frac{D_f}{L_f^2} \varphi_f = 0 \tag{B9}$$

Equations (B8) and (B9) will apply for passive regions if $K_f = K_{th} = 0$. At the interfaces between regions, the fluxes and neutron currents are continuous. At the extrapolated boundaries of the secondary reflector, the fluxes are zero.

Group Parameters

The constants required for solution of the two-group equations (B8) and (B9) in each region are:

(1) Fast: L_f^2, D_f, K_f, p_{th}

(2) Thermal: L_{th}^2, D_{th}, K_{th}

The validity of a group representation depends greatly on the correctness of the group constants used to represent the various competing

nuclear processes. Procedures used to evaluate group constants for highly enriched uranium hydrogeneous media are described in references 4 and 6 and are outlined in the following section.

Fast constants. - For neutrons slowing down in hydrogeneous media, the bulk of the contribution to L_f^2 is made at high neutron energies, that is, at energies above the epithermal region for which the inverse velocity variation of microscopic absorption cross section has reduced absorption to a negligible value. For highly enriched uranium systems, most of the absorption occurs in the epithermal region in the energy range below about 1000 electron volts. Hence, fast-group diffusion, leakage, and slowing-down processes may be effectively separated from epithermal absorption processes. If Fermi age theory is taken to apply in the epithermal region, the residual slowing-down, diffusion, and absorption processes in this region may be treated in detail. To accomplish this, neutrons should be divided into three separate groups: fast, epithermal, and thermal, as in references 4 and 6. All neutron absorption, and therefore production, is restricted to the epithermal and thermal regions. Group-diffusion slowing down in the fast region is then characterized by values of L_f^2 estimated from correlations of the few experimental metal-water-mixture measurements (ref. 4). Slowing down in the epithermal region is calculated by Fermi age theory, which provides the variation of neutron flux with energy to permit evaluation of the effective values of Σ_A, Σ_F, and p. These average values are obtained by weighting local values by the neutron flux in the epithermal region.

In the present two-group calculations, epithermal fissions and absorptions have been retained in the fast group, and the age-theory neutron slowing-down distribution in infinite media has been used to evaluate the fast-group constants. The fast constants D_f, K_f, and p_{th} are, therefore, obtained by weighting local values according to the energy distribution of neutron flux in an infinite medium of the same composition as the pertinent reactor region and as indicated by age theory. The fission spectrum is included in determining the energy distribution of neutron flux.

It is shown in reference 6 that a two-group formulation including epithermal absorption and fission predicts reactivities that agree with a formulation which considers in detail the energy-dependent nuclear processes in the epithermal region.

Thermal constants. - The thermal parameters are calculated from equations (B4) and (B7). Values of $\Sigma_{A,th}$ and $\Sigma_{F,th}$ are macroscopic cross sections obtained by averaging local values over the Maxwellian distribution of thermal neutron flux. The effects of thermal spectrum hardening due to preferential absorption in the lower energy portions of the thermal distribution have been neglected.

The diffusion coefficient D_{th} is given by the sum of the contributions of each constituent atom, the hydrogen atom usually being the largest contributor. The effects of the chemical binding of the hydrogen atom to the water molecule, however, significantly alter thermal scattering properties of hydrogen because of the increasing effective mass of the hydrogen atom for neutrons in the lower energy portions of the thermal distribution.

The effective value of D_{th} for any media is also obtained by averaging local values over the Maxwellian distribution of neutron flux, provided the variation of effective mass of the hydrogen atom with local energy is known. In the absence of these specific data, a method attributable to Radkowsky (described in ref. 7), which checks experimentally determined thermal diffusion properties of water for a range of temperature, was used. A value of 31.4 barns was obtained for the effective microscopic transport cross section for hydrogen. This value, which corresponds to an experimental value of thermal diffusion length of 2.80 centimeters in water at room temperature, has been used in the present calculations.

REFERENCES

1. Oak Ridge National Laboratory: Light-Water-Moderated Reactor. Type II - Heterogeneous-Enriched Fuel. TID 5275, ch. 2 of Research Reactors, Selected Reference Material - U.S. Atomic Energy Program, 1955. (Available from U. S. Govt. Printing Office.)

2. Grueling, E., Spinrad, B., and Masket, A. V.: Critical Mass and Neutron Distribution Calculations for the H_2O-Moderated Reactor with D_2O, H_2O and Be Reflectors. MonP-402, Clinton Labs., Monsanto Chem. Co., Oct. 29, 1947. (Contract W-35-058-eng.71.)

3. Dietrich, J. R., and Okrent, D.: Spatial Distribution of Heat Generation. Ch. 16 of The Reactor Handbook. Vol. 2 - Engineering. AECD 3646, U.S. Atomic Energy Comm., May 1955, pp. 87-121.

4. Deutsch, R. W.: Computing 3-Group Constants for Neutron Diffusion. Nucleonics, vol. 15, no. 1, Jan. 1957, pp. 47-51.

5. Spooner, Robert B.: Using a Reactor Simulator for Design Analysis. Nucleonics, vol. 12, no. 4, Aug. 1954, pp. 36-39.

6. Bogart, D., and Valerino, M. F.: Some Epithermal Effects on Criticality Requirements of Water-Moderated Reactors. TID 2014, Reactor Sci. and Tech., vol. 4, no. 3, Sept. 1954, pp. 107-114.

7. Chernick, J.: Theory of Uranium Water Lattices. Vol. V. A/Conf.8/P/603, International Conf. on the Peaceful Uses of Atomic Energy, June 30, 1955.

TABLE I. - TWO-GROUP DIFFUSION PARAMETERS

[Vertical buckling in all cases, $B_z^2 = 0.001622$.]

Reactor region	Fast group				Thermal group		
	D_f	L_f^2	K_f	p_{th}	D_{th}	L_{th}^2	K_{th}
Bulk Shielding Reactor core (0.423 Al, 0.577 H_2O, U^{235})	1.320	64.0	1.517	0.864	0.269	3.821	1.612
BeO reflector (0.876 BeO, .074 Al, .050 H_2O)	.783	117.5	-----	1.000	.563	242.0	-----
H_2O reflector	1.146	31.4	-----	.977	.160	8.189	-----

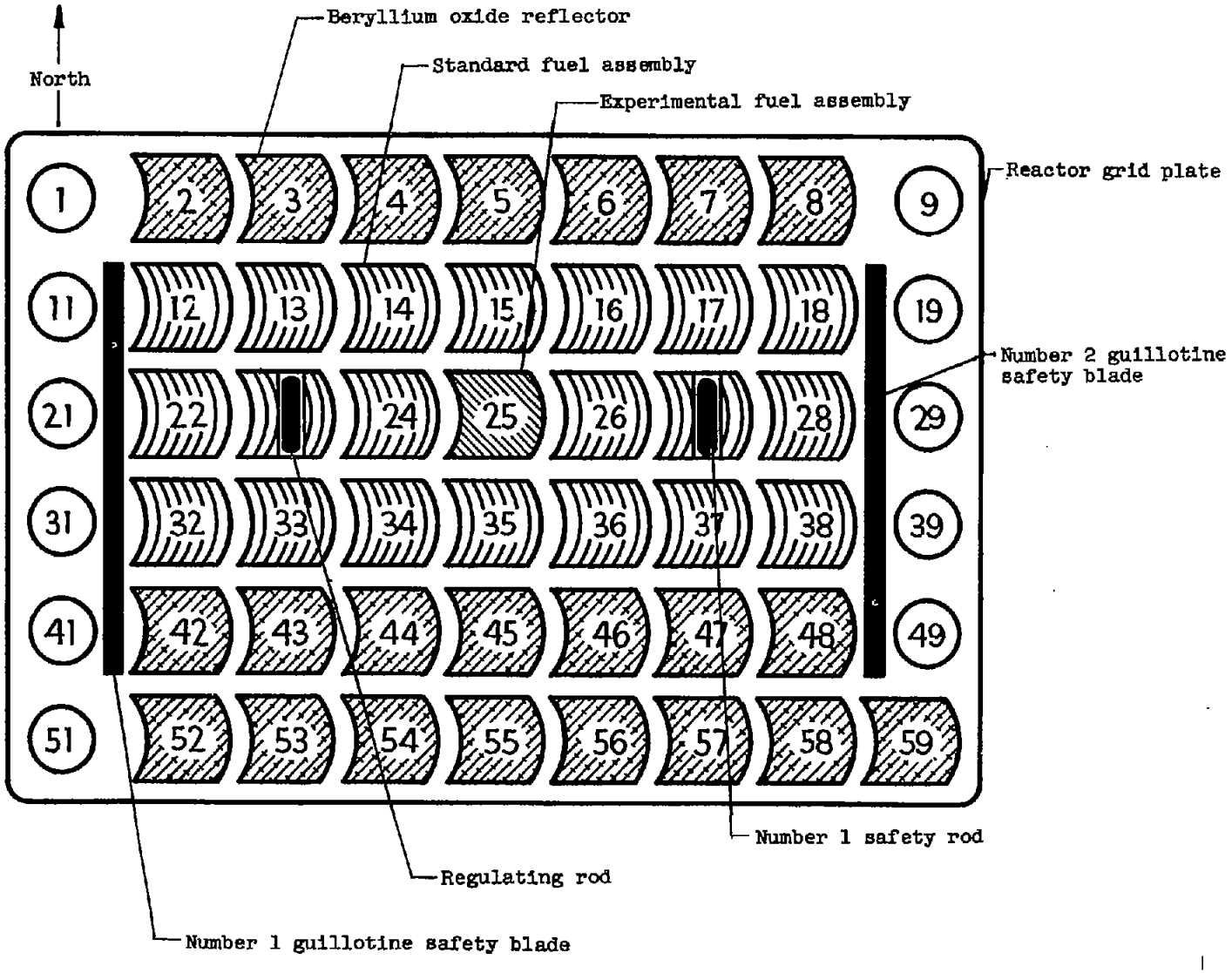

Figure 1. - Reactor loading for reactivity experiments at Bulk Shielding Reactor.

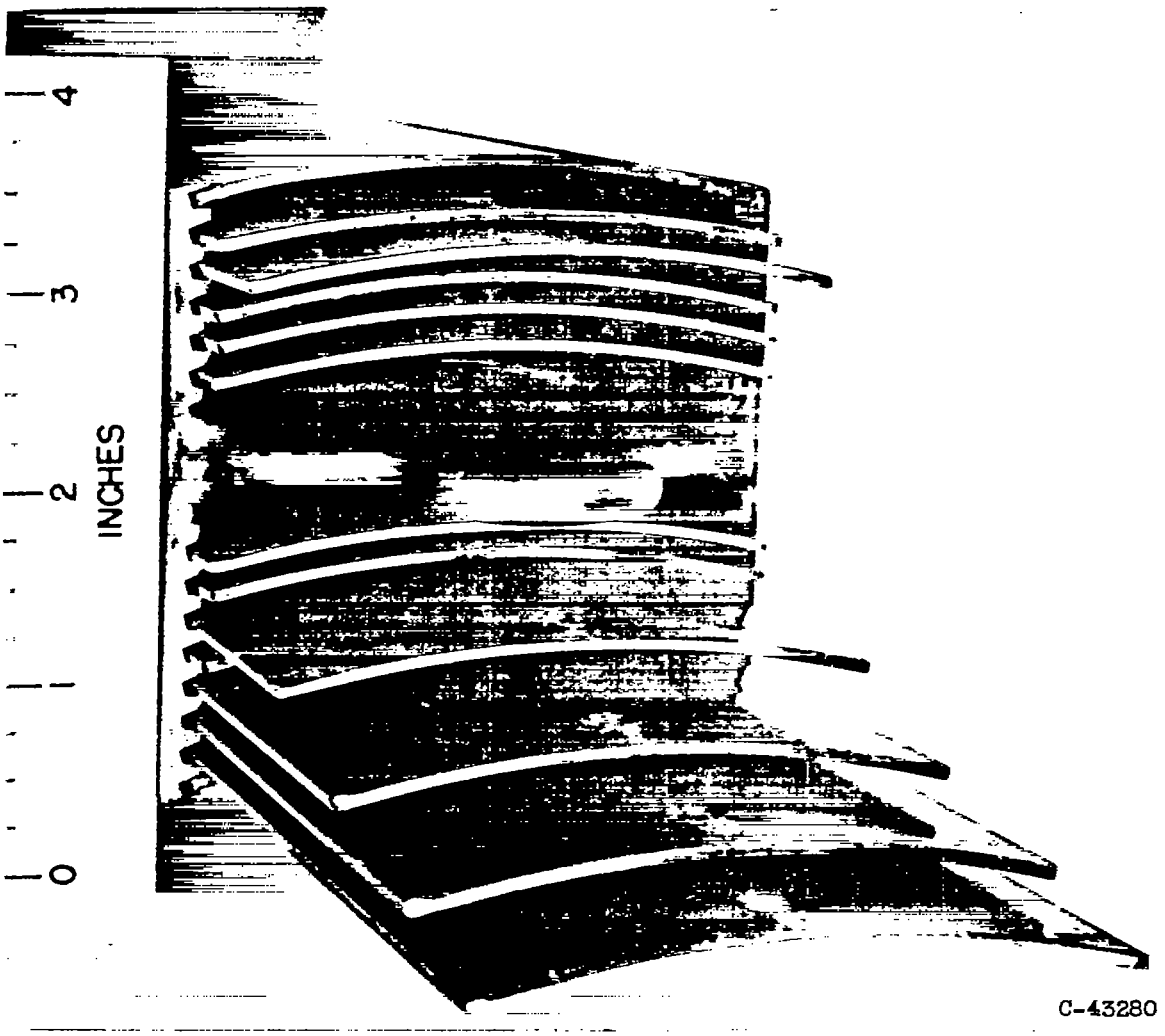

Figure 2. - Removable-fuel-plate element.

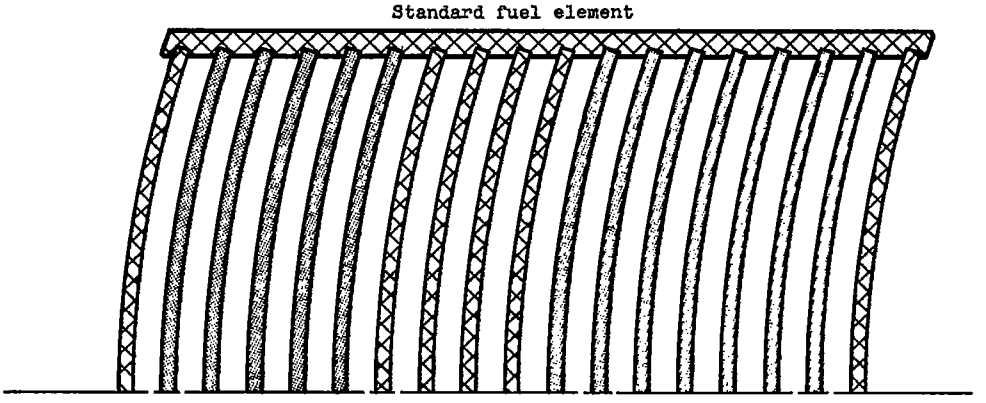

Step	Successive plates removed											
Maximum interaction (sequence I)												
1									J			
2									J	K		
3								I	J	K		
4							H	I	J	K		
5							H	I	J	K	L	
6						G	H	I	J	K	L	
7						F	G	H	I	J	K	L
8	A					F	G	H	I	J	K	L
9	A	B				F	G	H	I	J	K	L
10	A	B	C			F	G	H	I	J	K	L
11	A	B	C		E	F	G	H	I	J	K	L
12	A	B	C	D	E	F	G	H	I	J	K	L
Minimum interaction (sequence II)												
1	A											
2	A											L
3	A					F						L
4	A				E	F						L
5	A				E	F			J			L
6	A		C		E	F			J			L
7	A		C		E	F		H	J			L
8	A		C		E	F		H	J	K		L
9	A	B	C		E	F		H	J	K		L
10	A	B	C		E	F	G	H	J	K		L
11	A	B	C	D	E	F	G	H	J	K		L

Figure 3. - Sequences of removing fuel plates in standard fuel element of Bulk Shielding Reactor.

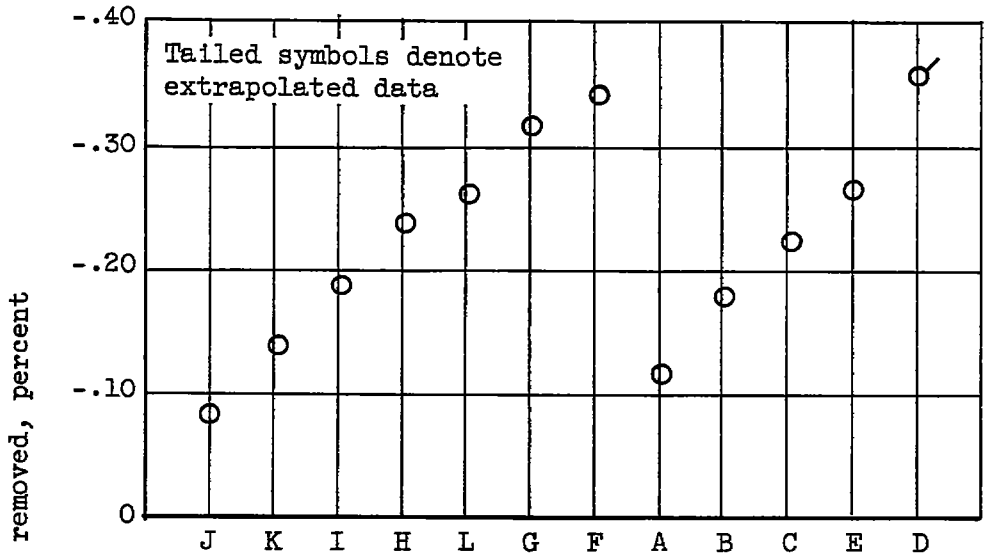

(a) Maximum interaction (sequence I).

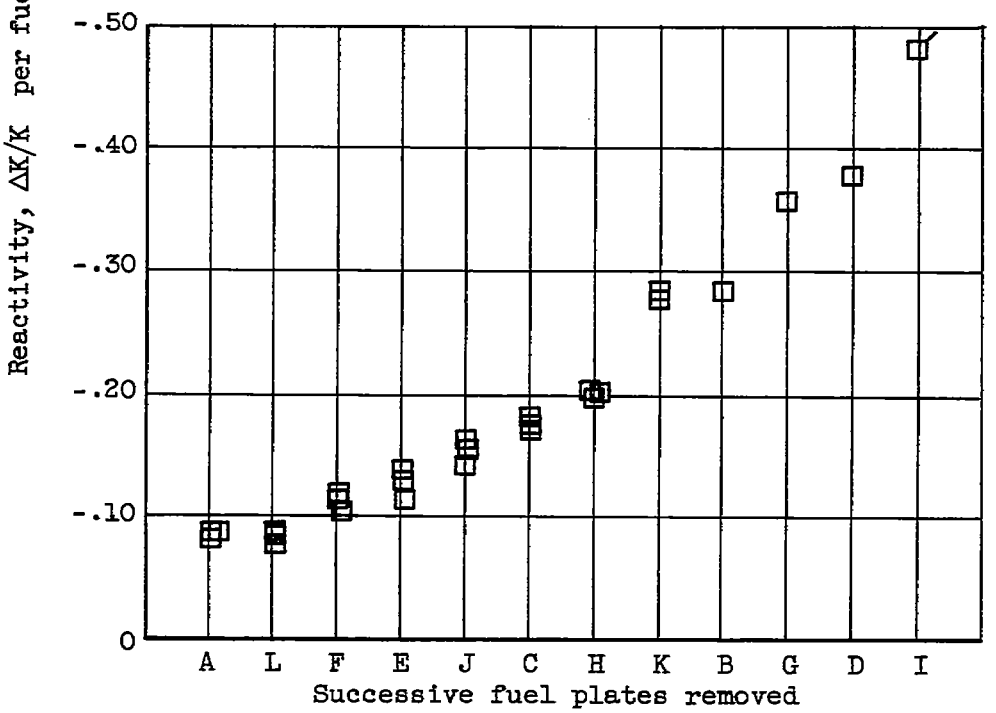

(b) Minimum interaction (sequence II).

Figure 4. - Reactivity for each fuel plate removed.

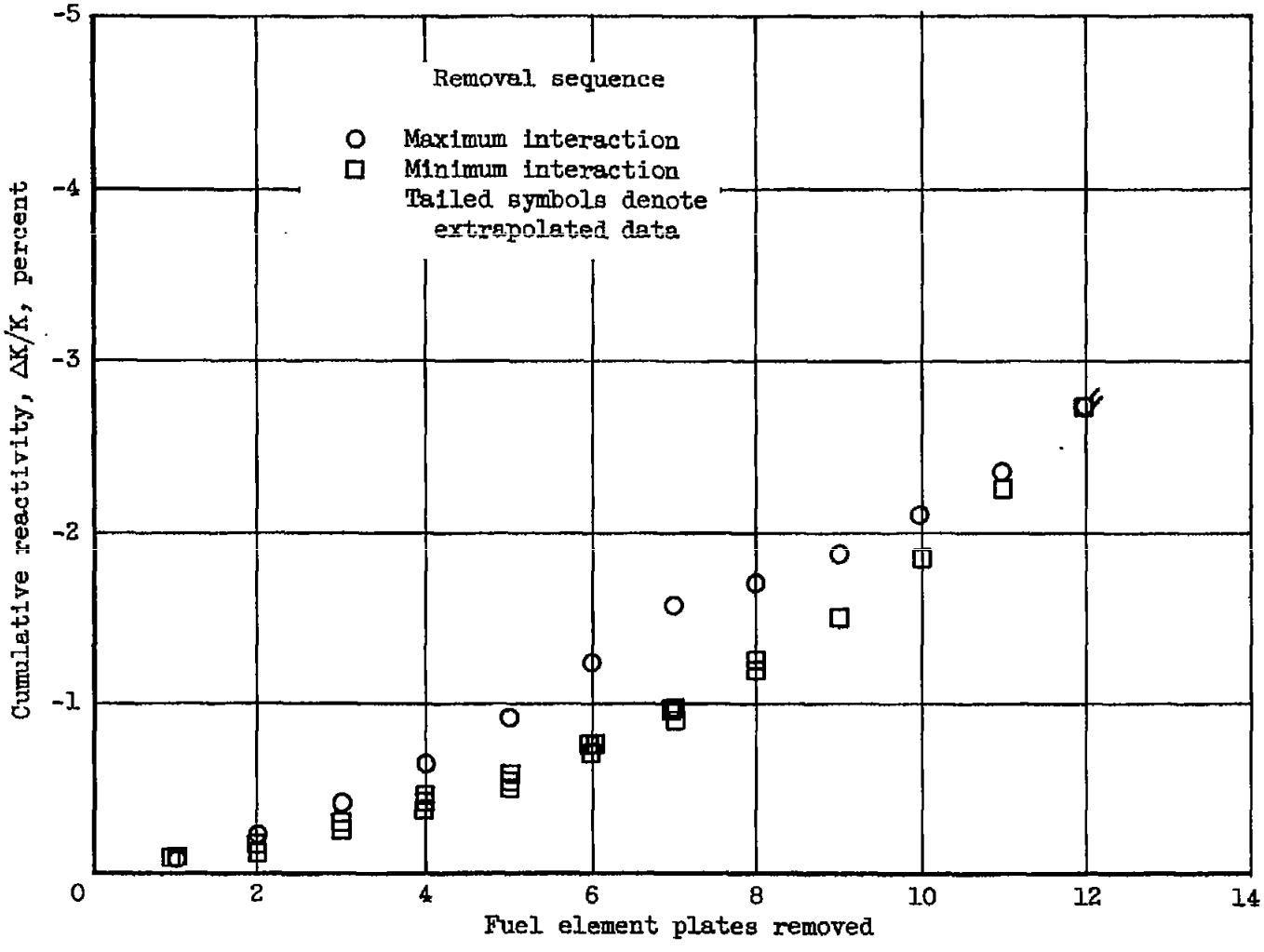

Figure 5. - Cumulative reactivity of fuel plates in element at grid position 25.

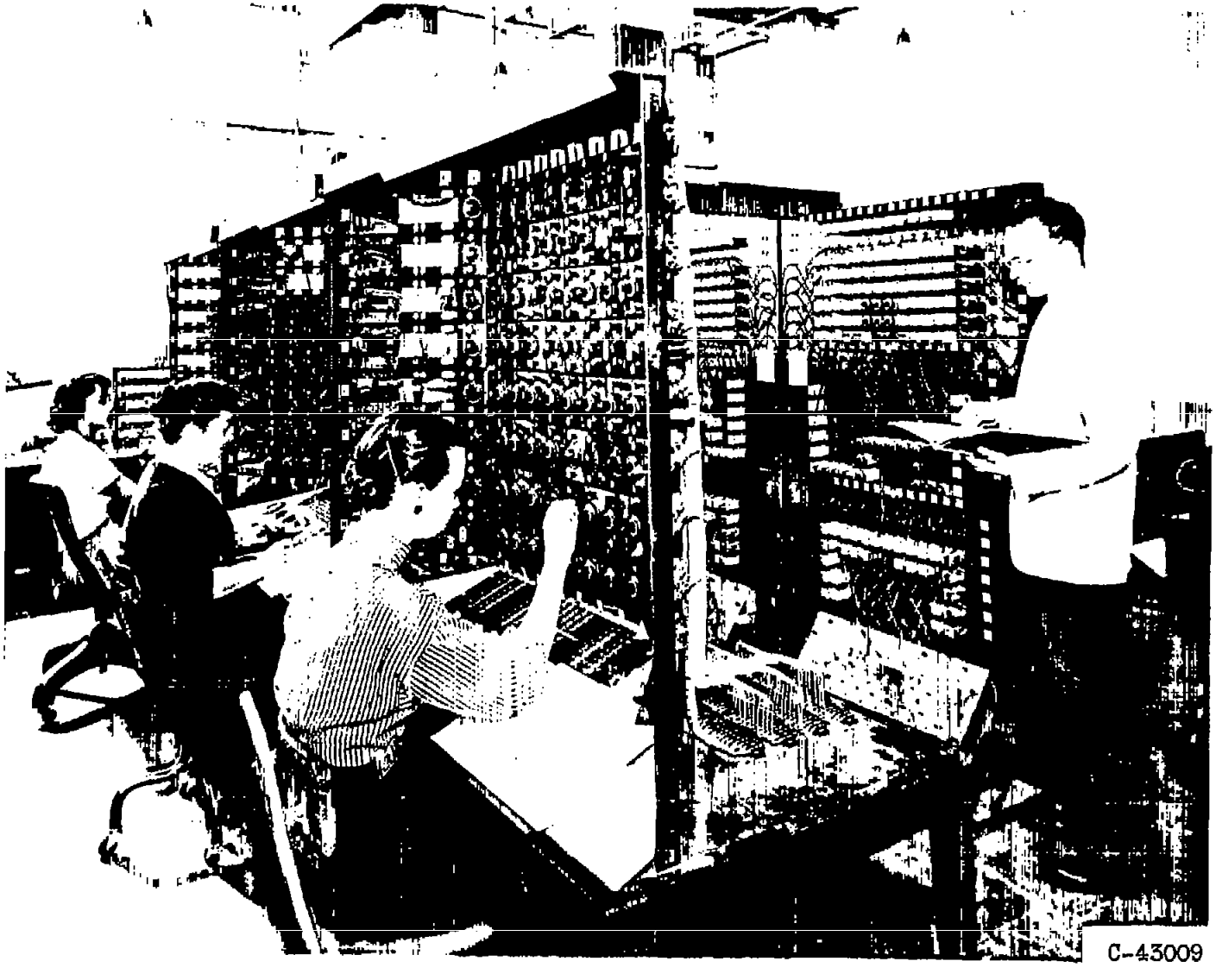

Figure 6. - Two-dimensional reactor simulator.

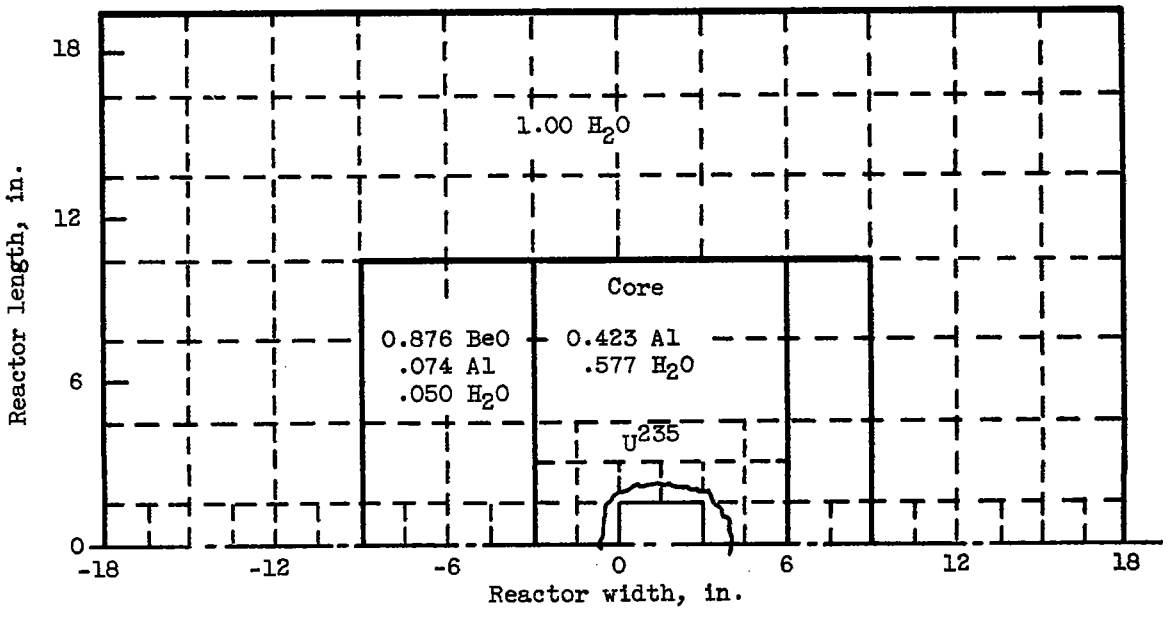

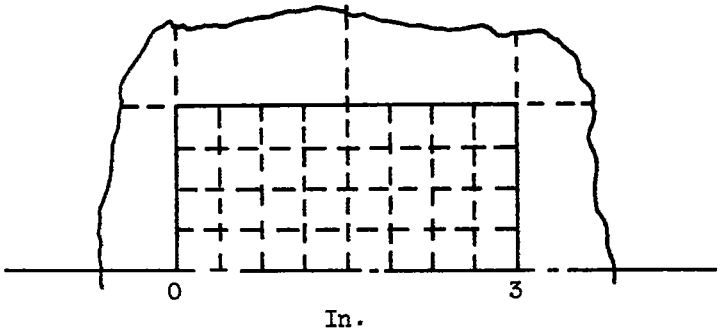

Figure 7. - Reactor geometry for two-dimensional simulator solutions.

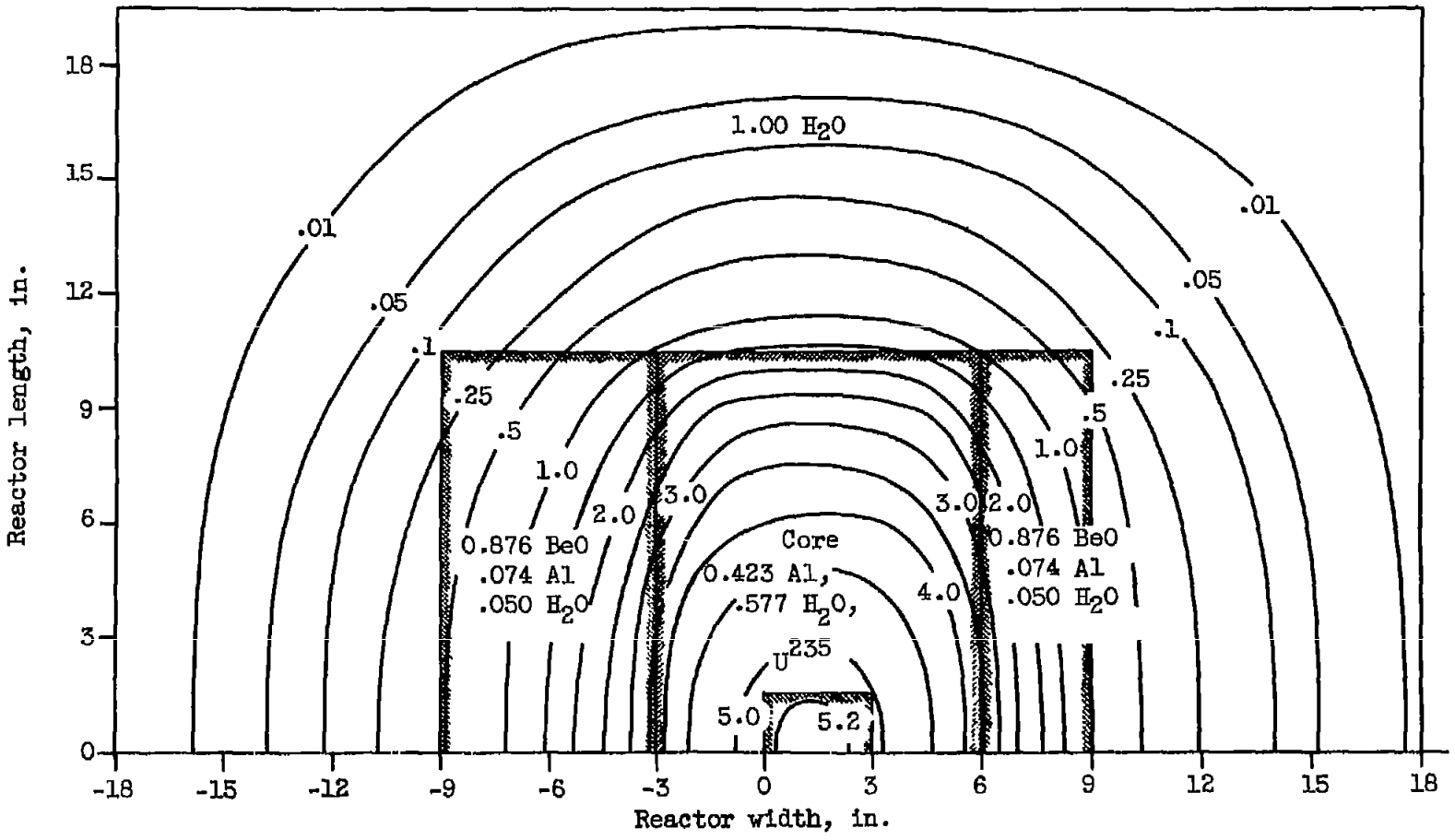

(a) Fast flux.

Figure 8. - Flux distribution for unperturbed core.

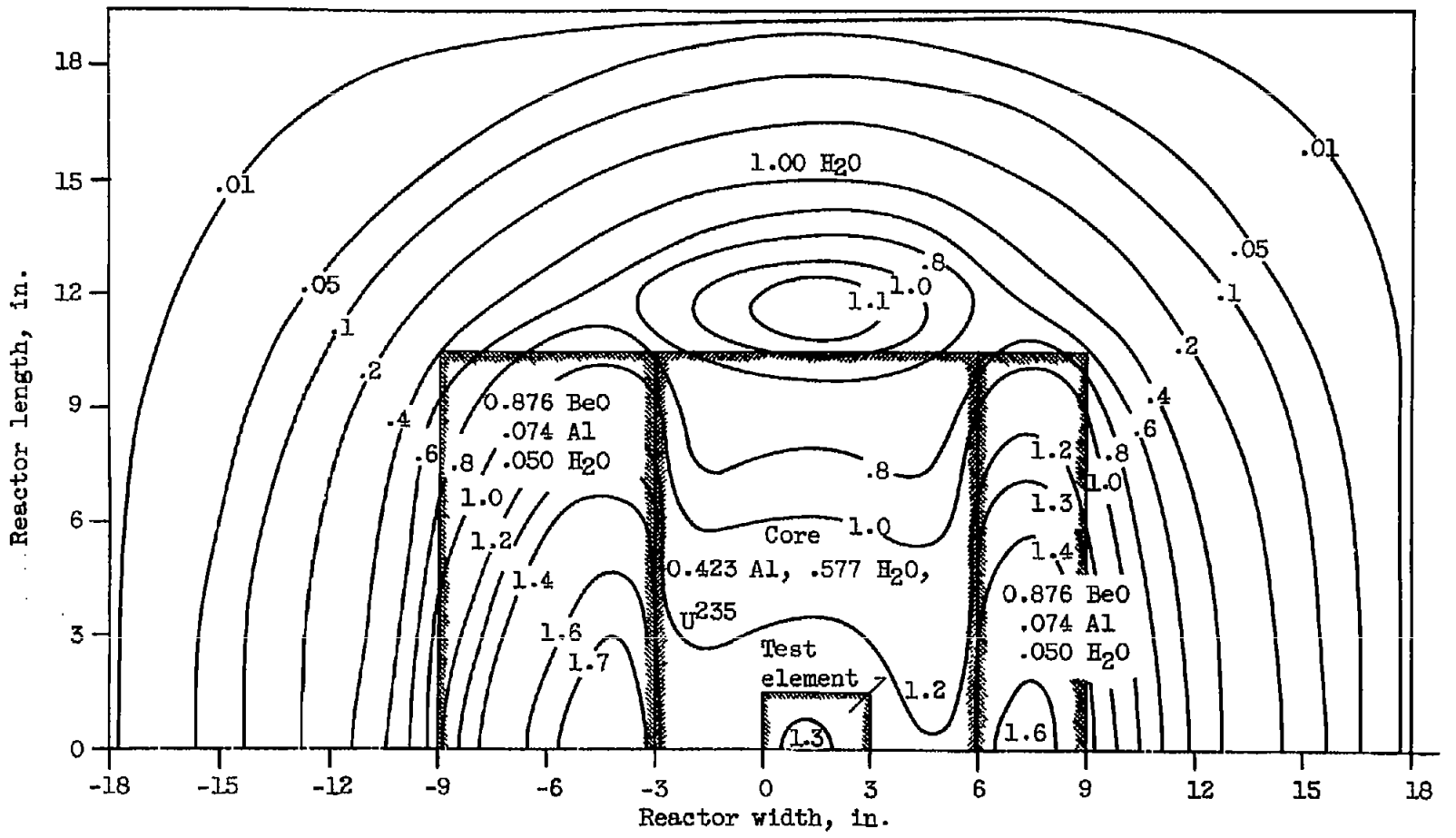

(b) Thermal flux.

Figure 8. - Concluded. Flux distribution for unperturbed core.

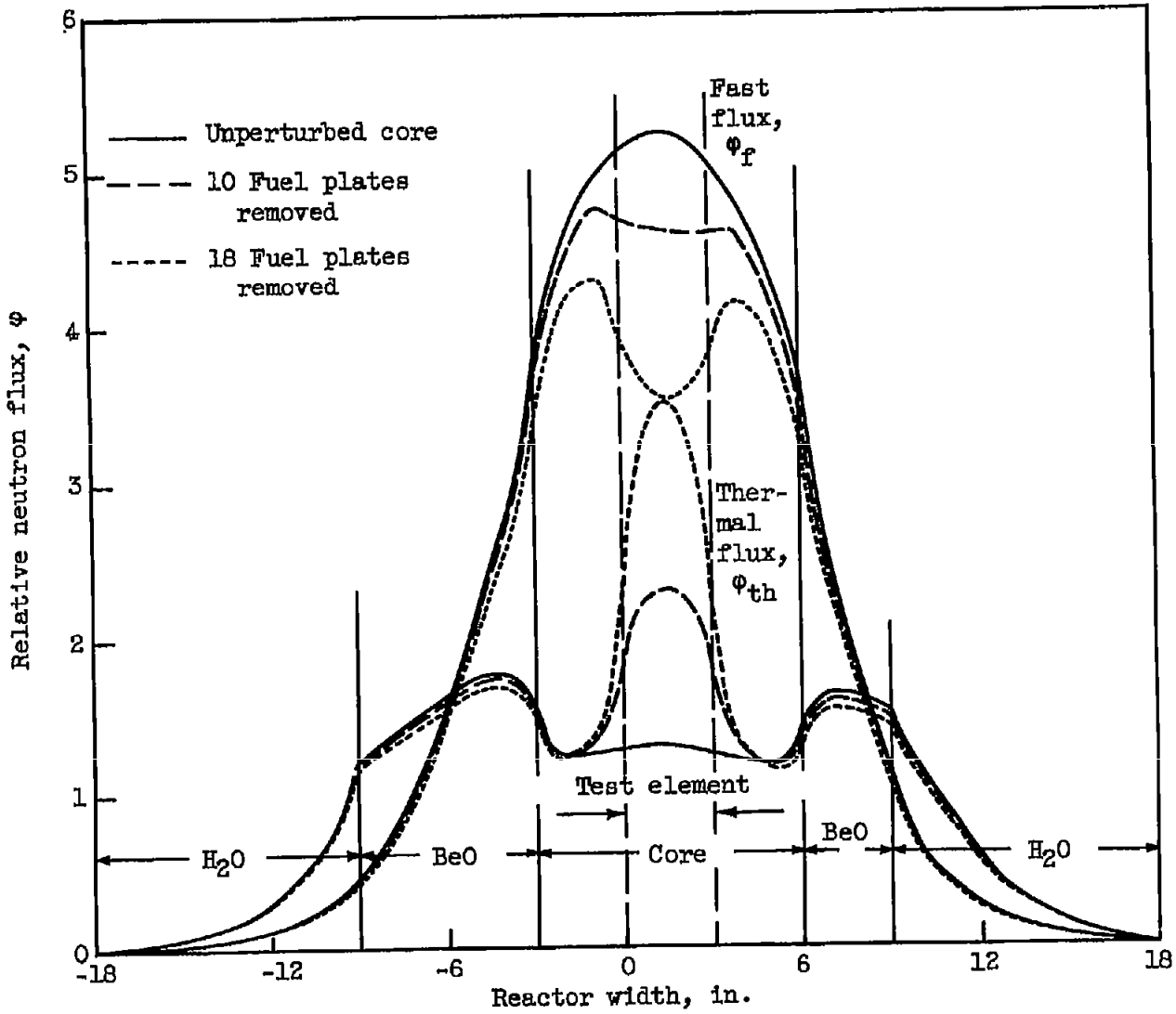

Figure 9. - Flux distributions along reactor width for local slowing-down cases.

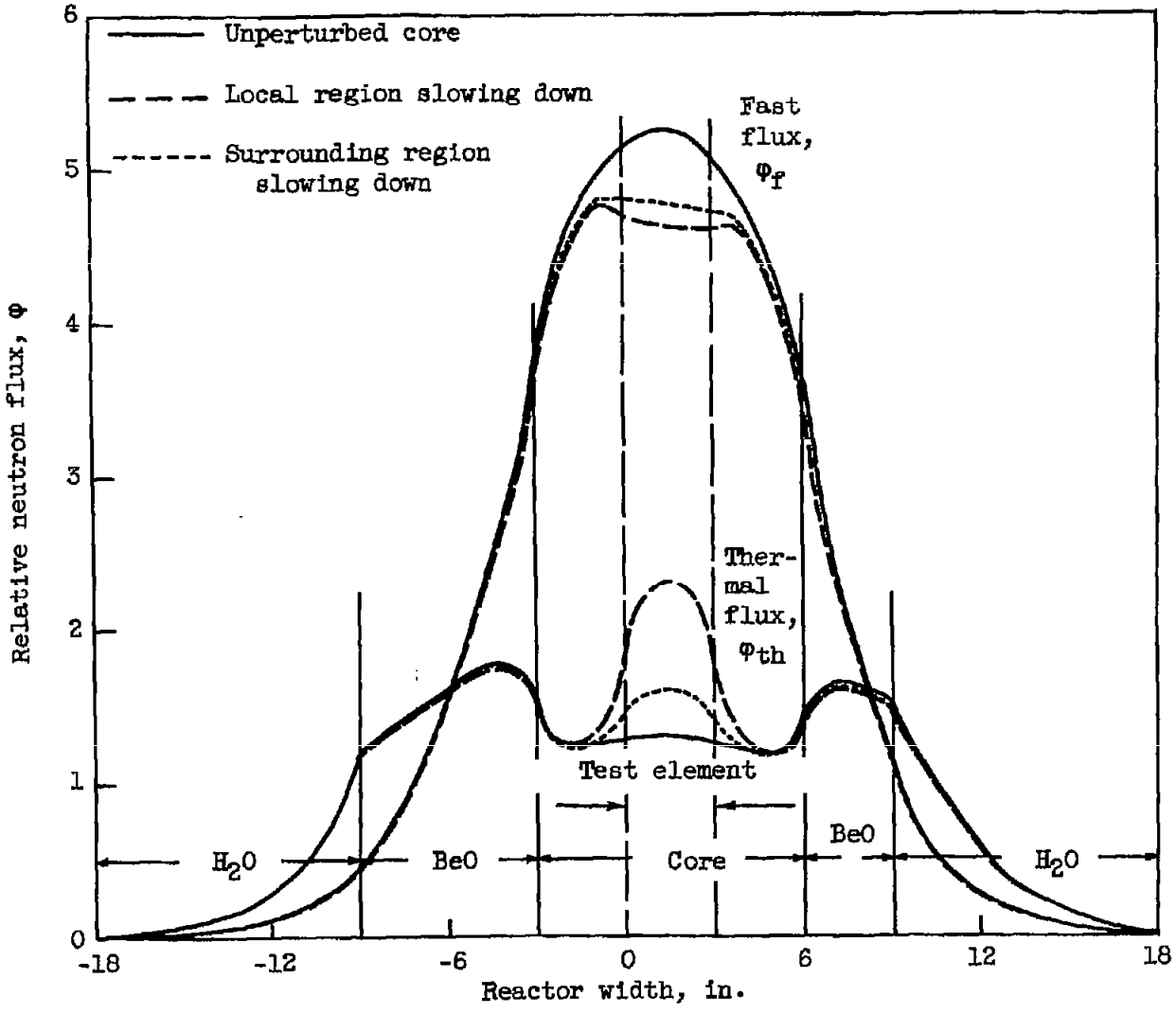

Figure 10. - Flux distributions along reactor width; slowing-down comparisons for cases with 10 plates removed.

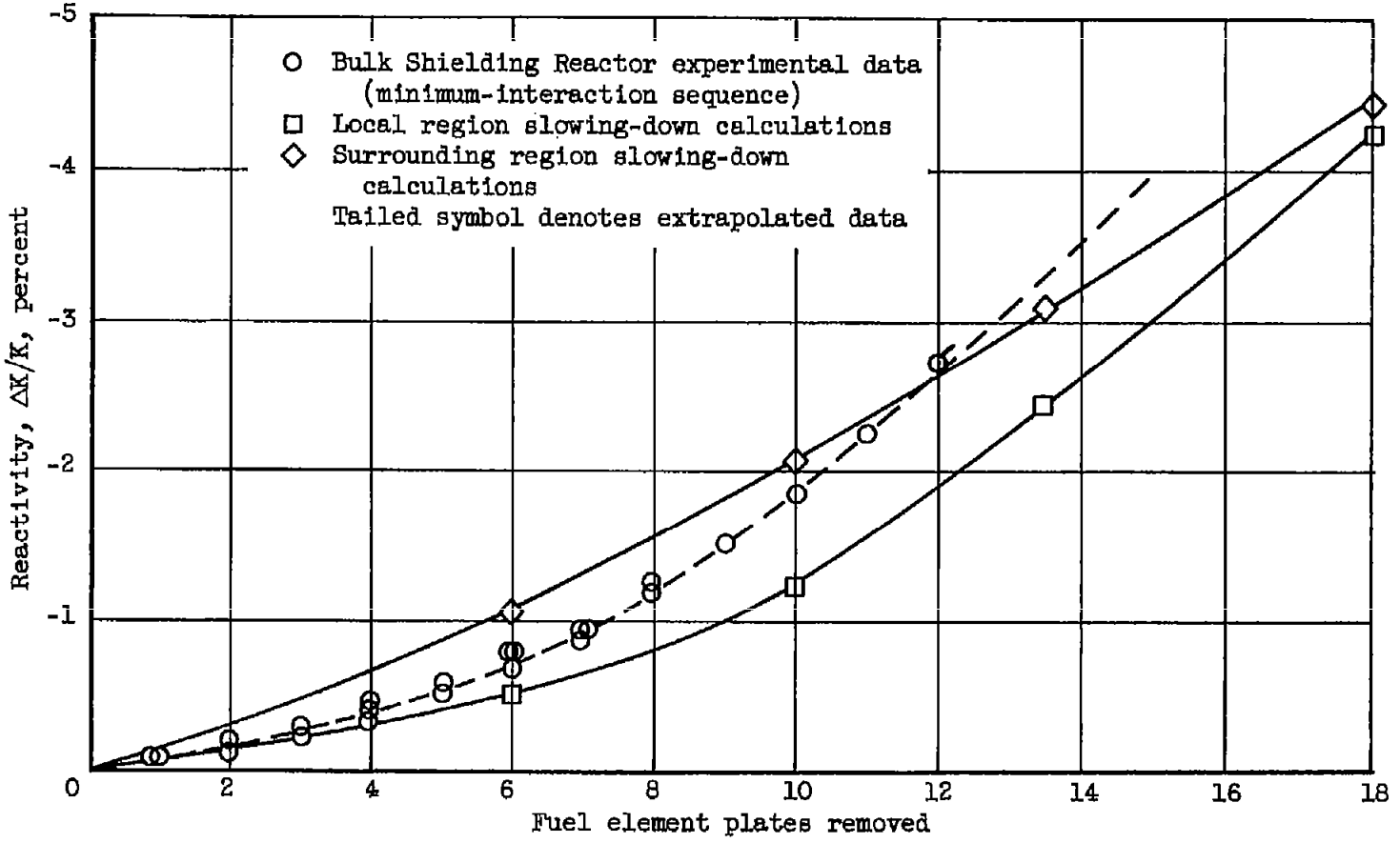

Figure 11. - Comparison of experimental and calculated reactivity effects of fuel-plate removal.

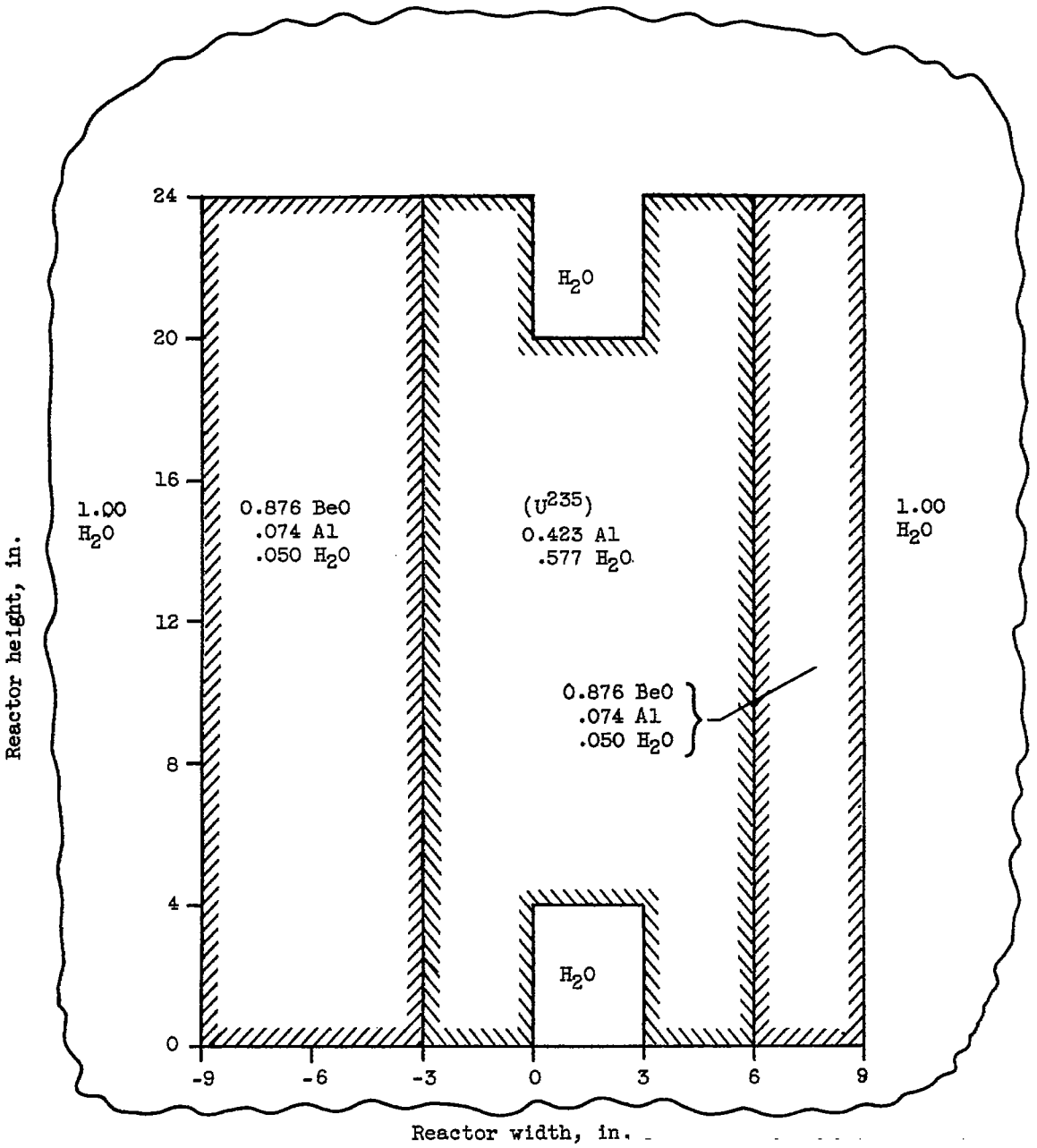

Figure 12. - Illustration of asymmetry due to water passage in core center.